Numerical Simulation of Dispersion of Volcanic CO_2 Seeped From Seafloor by Using Multi-Scale Ocean Model

Muneyasu Harata*, Toru Sato*, Shinichiro Hirabayashi*, Koichi Goto**
*Department of Ocean Technology, Policy, and Environment, University of Tokyo
5-1-5 Kashiwa-no-ha, Kashiwa, 277-8563 Japan
**Environmental Chemistry Department, The General Environmental Technos Co., Ltd.
1-3-5 Azuchimachi Chuo-ku Osaka, 541-0052 Japan

***Abstract*-Numerical simulations were conducted to predict the change of CO_2 concentration in the ocean caused by volcanic CO_2 seeped from the seafloor in Wakamiko Caldera in Kagoshima Bay. The behavior of CO_2 bubbles, their dissolution, and the advection-diffusion of dissolved CO_2 in the water column were numerically simulated. A multi-scale ocean model, in which hydrostatic meso-scale and non-hydrostatic small-scale models are combined, was used for this purpose. The calculated distribution of CO_2 concentration was in good agreement with observed data and the validity of the present multi-scale ocean model was confirmed.**

I. INTRODUCTION

Sub-seabed geological storage of CO_2 is one of the technologies for mitigating global warming. In this method, the main risk is the environmental impact caused by the leakage of sequestrated CO_2 from the seafloor and it is necessary to predict how the leaked CO_2 dissolves, diffuses, and finally evacuates into the atmosphere. Kano et al. [1] developed a two-phase flow model, by which the shapes and the phase change of CO_2 are considered, and carried out simulations on CO_2 leakage in an oceanic site off the Japanese coast. However, the validation of their model was not conducted.

In this study, we focused on an underwater caldera in Kagoshima Bay (Fig. 1), where CO_2 is naturally seeped by volcanic activities. Numerical simulations of dispersion of seeped CO_2 were carried out by using the two-phase flow model of Kano et al. [1], based on the measured physical properties, such as tidal current velocity, temperature, salinity, and background total CO_2 concentration (TCO_2). The purpose of this study is to validate the developed model by comparing the distribution of dispersed CO_2 between calculations and measurements, by reproducing the tidal currents in the whole Kagoshima Bay with its real topography.

II. OCEANIC MEASUREMENT IN KAGOSHIMA BAY

The oceanic measurements were carried out twice in different seasons in 2009. The first was from Jan. 26 to Feb. 10, which corresponds to the winter season with developed vertical mixing. The second measurement was from Sep. 7 to 11, which corresponds to the summer season with strong density stratification. Bottle sampling and CTD measurement were conducted in the observation points shown in Fig. 2, which denotes Wakamiko Caldera shown by a red square in Fig. 1, to obtain vertical distributions of temperature, salinity, and background TCO_2. Tidal velocity was also measured by using three three-dimensional (3D) acoustic Doppler

Figure 1. Survey points in Kagoshima Bay.

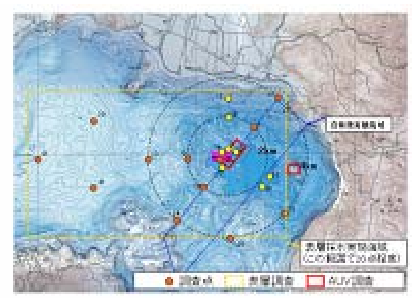

Figure 2. Survey points near and in Wakamiko Caldera.

This work was conducted as a part of the research project "the Investigating the Environmental Management System for Offshore CCS" of Japan NUS Co., Ltd. by the consignment of Ministry of the Environment, Japan.

978-1-4244-5222-4/10/$26.00 ©2010 IEEE

velocimeters (ADV) and an acoustic Doppler current profiler (ADCP) moored in the caldera.

III. Descriptions of Numerical Models

A. Mesoscale Ocean Flow Model

For mesoscale ocean model, a hydrostatic model with variable grids developed by the Marine Environmental Committee (MEC) [2] was applied. Its governing equations follow.

$$\frac{\partial u}{\partial t}=-u\frac{\partial u}{\partial x}-v\frac{\partial u}{\partial y}-w\frac{\partial u}{\partial z}+fv-\frac{1}{\rho_0}\frac{\partial p}{\partial x}+A_M\left(\frac{\partial^2 u}{\partial x^2}+\frac{\partial^2 u}{\partial y^2}\right)+\frac{\partial}{\partial z}\left(K_M\frac{\partial u}{\partial z}\right) \quad (1)$$

$$\frac{\partial v}{\partial t}=-u\frac{\partial v}{\partial x}-v\frac{\partial v}{\partial y}-w\frac{\partial v}{\partial z}-fu-\frac{1}{\rho_0}\frac{\partial p}{\partial y}+A_M\left(\frac{\partial^2 v}{\partial x^2}+\frac{\partial^2 v}{\partial y^2}\right)+\frac{\partial}{\partial z}\left(K_M\frac{\partial v}{\partial z}\right) \quad (2)$$

$$0=-\frac{1}{\rho_0}\frac{\partial p}{\partial z}-g \quad (3)$$

$$\frac{\partial u}{\partial x}+\frac{\partial v}{\partial y}+\frac{\partial w}{\partial z}=0 \quad (4)$$

where u, v, w are the velocity components in x, y, z directions, respectively, p is the pressure, ρ is the density of seawater, ρ_0 is its standard, g is the gravity acceleration, and A_M and K_M are coefficients of horizontal and vertical eddy viscosity, respectively.

B. Small-Scale Full-3D

In this study, a Multi-scale ocean model, in which the computational domain of a small-scale model is implemented in one cell of the horizontal plane of the MEC model, was adopted. In the small-scale model, two-phase flow was analyzed and its numerical solver should be non-hydrostatic (full-3D), since vertical flows entrained by rising bubble plumes cannot be ignored.

For simulating the dispersion of CO_2 seeped from seafloor, it is necessary to consider the continuous phase of seawater and the discrete phase of CO_2 bubbles separately. For this purpose, the gas-liquid two-phase Eulerian-Lagrangian model of Kano et al. [3] was adopted in this study. The governing equations for the continuous phase are the mass, momentum, and energy conservation laws:

$$\frac{\partial}{\partial t}(\alpha_c\rho_c)+\nabla\cdot(\alpha_c\rho_c\mathbf{u}_c)=\frac{1}{V_{cell}}\sum_{n=1}^{n_d}\Gamma, \quad (5)$$

$$\frac{\partial}{\partial t}(\alpha_c\rho_c\mathbf{u}_c)+\nabla\cdot(\alpha_c\rho_c\mathbf{u}_c\mathbf{u}_c)+\frac{1}{V_{cell}}\sum_{n=1}^{n_d}\frac{D_d}{Dt}(\rho_d V_d\mathbf{u}_d)=-\nabla P+\nabla\cdot\left[\alpha_c\rho_c(v_c+v_t)\mathbf{d}_c\right], \quad (6)$$

$$\frac{\partial}{\partial t}(\rho_c c_c T_c)+\nabla\cdot(\rho_c c_c T_c\mathbf{u}_c)=\nabla\cdot\left[\rho_c c_c\left(\kappa+\frac{v_t}{Pr_t}\right)\nabla T_c\right]+\Phi, \quad (7)$$

where

$$\alpha_d+\alpha_c=1, \quad (8)$$

$$\alpha_d=V_{cell}^{-1}\sum_{n=1}^{n_d}V_d, \quad (9)$$

$$\mathbf{d}_c=\nabla\mathbf{u}_c+(\nabla\mathbf{u}_c)^T, \quad (10)$$

$$\Phi=\tfrac{1}{2}\rho_c v_c\,\mathbf{d}_c:\mathbf{d}_c, \quad (11)$$

where α is the volume fraction, $\mathbf{u}$ is the velocity vector, n_d is the number of bubbles in a computational cell, V is the volume, V_{cell} is the volume of a computational cell, Γ is the mass transfer from a bubble at the interface, P is the pressure, Pr_t is the turbulence Prandtl number, κ is the thermal diffusivity, v is the kinematic viscosity, v_t is the eddy viscosity, and the subscripts, c and d, denote the continuous water phase and the dispersed CO_2 bubble phase, respectively. ρ_d and ρ_c are given by Pitzer and Sterner [4] and Alendal and Drange [5], respectively, and v_t is determined by the Smagorinsky's model [6].

For the dispersed phase, the mass conservation and the motion equations of bubbles are solved for each individual bubble:

$$\frac{D_d}{Dt}(\rho_d V_d)=-\Gamma, \quad (12)$$

$$\frac{D_d}{Dt}\left[(\rho_d+\beta\rho_c)V_d\mathbf{u}_d\right]=V_d\left[-\nabla P+(\rho_c-\rho_d)\mathbf{g}-\mathbf{f}_D-\mathbf{f}_L\right], \quad (13)$$

where

$$\mathbf{f_D}=\frac{1}{2}C_D\frac{3}{2d_e}\rho_c|\mathbf{u}_r|\mathbf{u}_r, \quad (14)$$

$$\mathbf{f_L}=C_L\rho_c\mathbf{u}_r\times\boldsymbol{\omega}_c, \quad (15)$$

$$\mathbf{u}_r=\mathbf{u}_d-\mathbf{u}_c, \quad (16)$$

$$\boldsymbol{\omega}_c=\nabla\times\mathbf{u}_c, \quad (17)$$

where β is the coefficient of added mass of a bubble, $\mathbf{g}$ is the gravity vector, $\mathbf{f_D}$ is the drag force acted on a bubble, $\mathbf{f_L}$ is the lift force acted on a bubble, C_D is the drag coefficient of a

TABLE I
MOLE FRACTION OF COMPONENTS IN GAS

Gas component	Mole fraction
CO_2	88.4×10^{-2}
N_2	8.7×10^{-2}
CH_4	2.9×10^{-2}

bubble, C_L is the lift coefficient of a bubble, d_e is the equivalent diameter of a bubble, $\mathbf{u}_r$ is the relative velocity of the dispersed phase to the continuous phase, and $\boldsymbol{\omega}_c$ is the vorticity of a bubble. β and C_L are both set to be 0.5. C_D is modeled later in this section. The models for C_D and Γ are given by Kano et al. [3].

Although Kano et al. [1] assumed the composition of bubbles was 100% CO_2, the composition of volcanic gas is known from the report of Kikawada et al. [7], which was adopted in this study and shown in Table I. Therefore, the discrete phase calculation was modified to treat the change in mole fraction of the mixed gas of CO_2, N_2, and CH_4. It was assumed that only CO_2 out of the three composites can dissolves in seawater.

IV. Results

Figure 3 shows the computational grids of Kagoshima Bay. Spin-up calculations of hydrostatic model were conducted for 15 days to represent tidal current field in Kagoshima Bay for the summer and winter seasons. Results were compared with the observation and the appropriate boundary condition of tidal elevation was determined by trial and errors. The initial and boundary conditions of the vertical distribution of temperature, salinity, and TCO_2 were given by the measurement. After the spin-up calculation, the dispersion of seeped CO_2 was calculated for 15 days.

A. *Winter Season*

The temporal change in calculated tidal elevation in the winter season reproduced by the spin-up calculation is shown in Fig. 4 in comparison with the observational data. These data were monitored at a tide observatory in the narrow channel near the head of the bay. The calculated result agreed well with the observation and it can be said that the flow field in Kagoshima Bay was properly represented by the present method.

The seepage amount of CO_2 in the dispersion simulation was set to be 48500 ton/year, which was estimated from the difference in the measured mass of CO_2 between the two seasons, based on the assumption that dissolved CO_2 never goes out from the seasurface due to the strong stratification in the summer season and so does in the winter. It is considered that CO_2 seeped from seafloor is in the forms of gas bubble and mass flux dissolved in sediment water. Because their ratio is unknown, three cases of dispersion simulations with different ratios, as listed in Table II, were carried out.

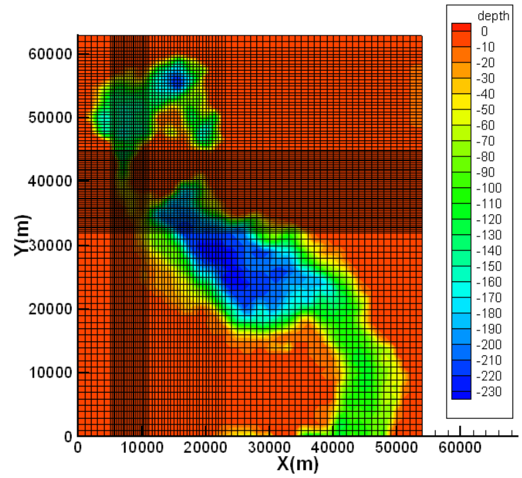

Figure 3. Computational grid in Kagoshima bay.

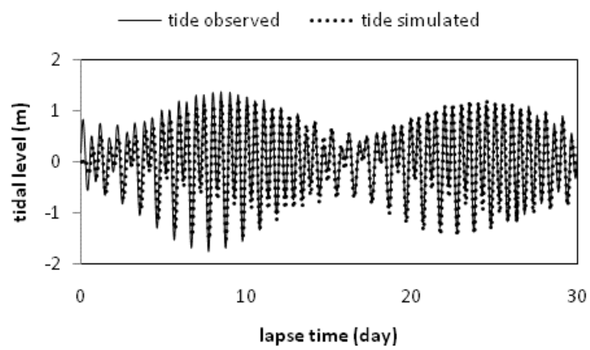

Figure 4. Comparison in temporal change in tidal elevation in winter between calculation and observation.

Figure 5 shows the vertical profiles of calculated and observed TCO_2 in the caldera in the three cases with different ratios in the seepage form. It is found that the result in Case 3 shows the best agreement with the observation among the three cases. Figure 6 shows the contour maps of calculated and observed TCO_2 on a South-North vertical section in Wakamiko Caldera in Case 3. Figure 7 shows the velocity vectors on the same vertical section in the caldera 15 days after the start of the dispersion calculation in Cases 1 and 3. It is considered from these figures that the development of vertical velocity entrained by rising bubbles makes the difference in vertical mixing of TCO_2.

TABLE II
RATIO OF LEAKED CO_2 IN BUBBLE FORM OR DISSOLVED FORM.

	Ratio (bubble)	Ration (flux)
Case1	10	0
Case2	7	3
Case3	5	5

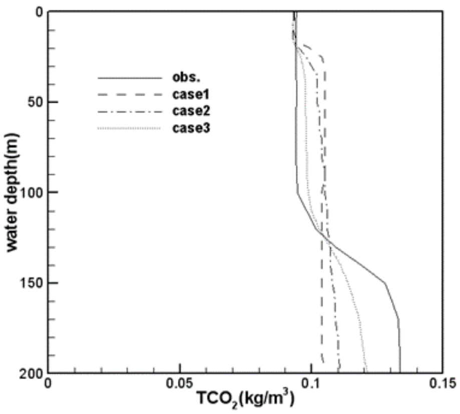

Figure 5. Vertical profiles of TCO_2 in winter in Wakamiko Caldera.

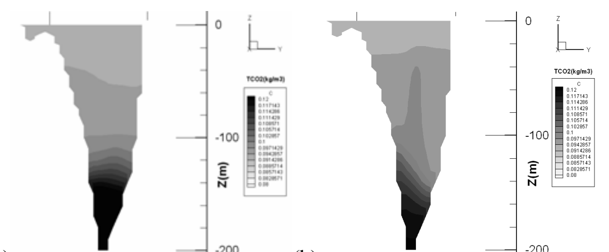

(a) (b)
Figure 6. Contour maps of observed (a) and calculated (b) TCO_2 in winter in Wakamiko Caldera in winter in Case 3.

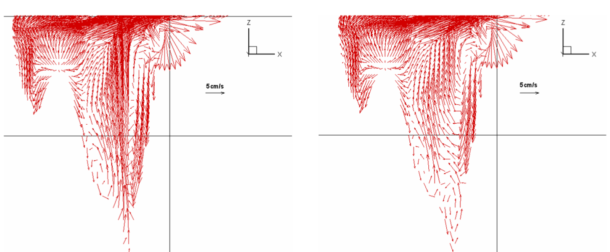

(a) (b)
Figure 7. Velocity vectors in winter in Wakamiko Caldera in Case 1 (a) and Case 3 (b).

B. *Summer Season*

Figure 8 shows the temporal change in tidal elevation in the spin-up calculation in comparison with the observational data for the summer season. Good agreement can be seen.

The vertical profiles of calculated and observed TCO_2 in the caldera are shown in Fig. 9. Figure 10 shows the contour maps of calculated and observed TCO_2 in Case 3. It is found that the calculated results agreed well with the observations in all the cases and no significant difference can be found among the three cases, unlike the tendency seen for the winter season (Fig. 5).

In order to analyze the difference between summer and winter seasons, velocity vectors in the caldera 10 days after the start of dispersion calculation was shown in Fig. 11. It is found that the upwelling flow entrained by the rising bubbles does not reach the surface because of the existence of

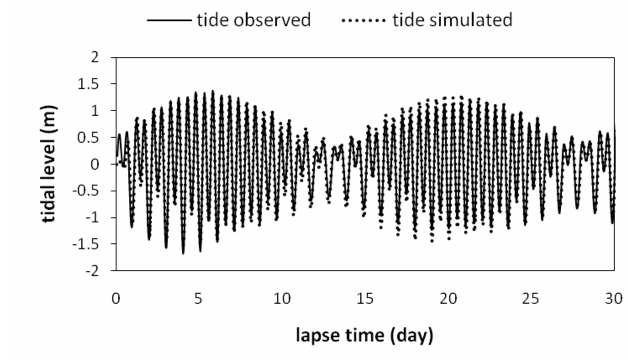

Figure 8. Comparison in temporal change in tidal elevation in summer between calculation and observation.

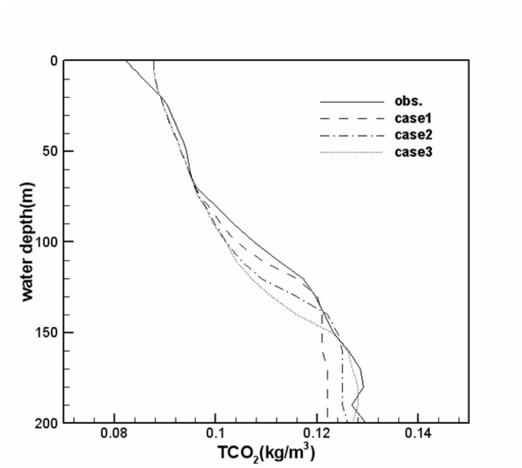

Figure 9. Vertical profiles of TCO_2 in summer in Wakamiko Caldera.

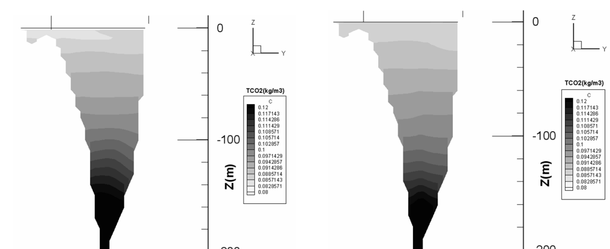

(a) (b)
Figure 10. Contour maps of observed (a) and calculated (b) TCO_2 in summer in Wakamiko Caldera in winter in Case 3.

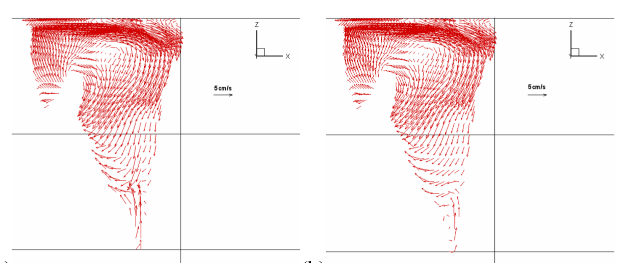

(a) (b)
Figure 11. Velocity vectors in summer in Wakamiko Caldera in Case 1 (a) and Case 3 (b).

horizontal flows above the caldera. It is considered that the vertical upwelling is blocked in summer and TCO_2 in the caldera is maintained almost constant regardless of the ratio of the seepage forms.

V. Concluding Remarks

Dispersion of CO_2 seeped from Wakamiko Caldera in Kagoshima Bay was numerically simulated for two seasons of winter and summer and their results were compared with field data obtained in the real sea. In the flow calculation, the temporal changes in tidal elevation showed good agreements with the observations for the both winter and summer. It was also found that vertical mixing in winter and strong density stratification in summer were well simulated. In the calculation of CO_2 dispersion, three cases with different ratios of seepage form, i.e. gas bubbles and mass fluxes dissolved in sediment water, were considered. It is found that the case with the ratio of 5:5 showed the best agreement with the observation for the winter season. For the summer season, on the other hand, little difference can be found among the three cases due to the existence of strong stratification and the calculated TCO_2 distribution was well compared with the observation. It is fare to say that these facts evidenced the validity of the present numerical method.

References

[1] Y. Kano, T. Sato, J. Kita, S. Hirabayashi, S. Tabeta, "Multi-scale modelling of CO_2 dispersion leaked from seafloor off Japanese coast", *Marine Pollut. Bull.* vol. 50, pp.215-224, 2010.

[2] T. Sato, K. Tonoki, Y. Tsuchiya, "Numerical and hydraulic simulations of effect of density current generators in semi-enclosed tidal bays", *Coastal Engrg.* vol. 53, pp. 49-64, 2006.

[3] Y. Kano, T. Sato, J. Kita, S. Hirabayashi, S. Tabeta, "Model prediction on the rise of pCO2 in uniform flows by leakage of CO2 purposefully stored under the seabed", *Int. J. Greenhouse Gas Control*, vol. 3, pp. 617-625, 2009.

[4] Pitzer, K.S., Sterner, S.M. 1994. Equations of state valid continuously from zero to extreme pressures for H2O and CO2. Journal of Chemical Physics 101: 3111-3116.

[5] Alendal G., Drange, H. 2001. Two-phase, near-field modeling of purposefully released CO2 in the ocean. Journal of Geophysical Research 106(C1): 1085-1096.

[6] Smagorinsky, J. 1993. Some historical remarks on the use of nonlinear viscosities. In Galperin, B. and Orszag, S.A. (eds.) Large eddy simulation of complex engineering and geophysical flows. Cambridge University Press. ISBN 0-521-43009-7. pp. 3-36.

[7] Y. Kikawada, J. Kosaka, T. Oi, J. Hashimoto, "Chemical compositions of volcanic gases from submarine fumaroles in Wakamiko Caldera, northern Kagoshima Bay, Japan", *J. Balneological Soc. Japan*, vol. 57, pp.30-41, 2009 (in Japanese).